Journal of the Korean Nuclear Society
Volume 25, Number 1, March 1993

A Study on the Local Boiling of the Consolidated Spent Fuel Storage Pool

Chang Ju Lee
Korea Institute of Nuclear Safety

Kun Jai Lee
Korea Advanced Institute of Science and Technology

(Received April 16, 1991)

조밀화된 사용후 핵연료 저장조에서의 국부 비등에 관한 연구

이창주
한국원자력안전기술원
이건재
한국과학기술원

(1991. 4. 16 접수)

Abstract

The natural convection model of the consolidated system has been developed to make sure the removal of decay heat generated in the spent fuel for the loss of forced cooling accident. The numerical technique employed was based on the ADI scheme. The calculation of heat generation rate in the spent fuel was performed by the ANS-79 decay heat model, and the nonuniform surface heat flux is assumed with a chopped sine curve for the conservative decay heat generation input. The sensitivity study was performed to examine the possibility of the pool bulk boiling by varying the various parameters, i.e. inter-fuel spacing ratio, heat generation power, and radius of the fuel rod. The application results of this model show that the natural circulation flow through compacted spent fuel bundles enables the pool temperature to control in a safe and effective manner, after the required cooling time. The corresponding acceptance criteria of the cooling time for rearranging the spent fuel rods were also found.

요 약

강제순환 냉각상실사고시 조밀화된 저장계통의 사용후 핵연료에서 생성된 붕괴열의 제거를 확인하기 위한 자연순환 해석모델이 개발되었다. 채택된 수치기법은 ADI방법에 근거하였다. 사용후 핵연료의 붕괴열 생성율은 ANS-79 붕괴열 모델에 따라 계산되었으며, 보수적인 붕괴열 생성량 입력을 위해 chopped sine곡선에 따른 비균일 표면열속이 가정되었다. 저장조내 국부비등의 발생 가능성을 조사하기 위해서 민감도분석이 수행되었으며, 이는 핵연료간 거리비, 열 생성량 및 핵연료봉 반지름 등의 여러 변수를 변경시킴으로서 이루어졌다. 이 모델의 적용결과는 적절한 냉각시간 후의 조밀화된 사용후 핵연료 다발을 통한 자연대류 유량이 안전하고 효과적인 방식으로 저장조의

온도준위를 조절할 수 있음을 보여주고 있으며, 또한 사용후 핵연료봉 재배치를 위한 냉각시간에 관한 허용기준이 얻어졌다.

1. Introduction

With the current limitation or slow expansion on nuclear spent fuel reprocessing and the pre-allocated interim storage size, the storage capacity of spent fuels in the nuclear site pool requires the increased space. To accommodate the growing need of treatment capacity for spent fuel bundles, existing storage racks have been enlarged and adapted to higher densities by using the methods such as reracking, maximum density rack, and rod consolidation.[1,2] Among these at-reactor storage expansion techniques, the rod consolidation method might be a principal option for more efficient utilization of existing interim spent fuel water storage basins. It is to disassemble the spent fuel assembly and treat the structural materials as low level wastes except fuel rods, and rearrange the fuel rods into more compacted state. Rod consolidation thus can double the effective storage capacity with properly designed spent fuel racks. One of the major fields for the implementation of this advanced storage method is a site specific feasibility or safety study. In order to verify the means of increasing the interim storage capacity, the safety assessment must be performed in the various viewpoints including the areas of thermo-hydraulics, structural capability, criticality, shielding and so on.[3]

This study is interested in the thermo-hydraulic standpoint, particularly decay heat removal capability by the natural convection flow, of the consolidated storage design in the spent fuel pool. The safety function of the spent fuel pool and storage racks is to maintain the spent fuel assemblies in a safe array during all credible storage conditions. It is also performed by the pool cooling system, in all cases remains the same, that is, the spent fuel assemblies must be cooled and covered with water during all storage conditions. [4] A.S. Benjamin et al. analyzed a natural convection to determine the heatup of spent fuel following loss of water in the typical storage system. [5] M. E. Weech analyzed a natural convection phenomena in the high density racks and multi-element baskets. [6] Recently, the thermal analyses for the consolidated fuel rod storage have been performed by several authors. [7-9] The authors made an judgement on the capability of the spent fuel storage systems whether to provide adequate cooling and the proper time required for most operating and accident conditions.

It is assumed that the accident can be initiated from the failure of the pool cooling system and a single active failure is not accounted for that case, so the heat removal is achieved only by natural convection flow in the pool. The heat generated by the spent fuel is delivered to the pool water and cause the pool temperature increase until the generation of decay heat is balanced by the heat dissipation from the rod surface and wall of the pool. Because the other subchannel analysis schemes, such as COBRA[10] or THINC[11] series, are carried out by using the averaged values to the critical parameters, they can lead much uncertainties to predict the heat transfer mechanism, so they are not adequate to evaluate the impact of primitive variables in the compacted rod arrays. The three-dimensional calculation is, therefore, explicitly required. The evaluation of the natural convection heat transfer was based upon the coupled conservation equations of mass, momentum, and energy for the typical fuel element. A computational scheme was formed into the TASFIS(Thermohydraulic Analysis in Spent Fuel Interim Storage) code, which was developed

for this study only, to simulate the PWR standard spent fuel array system in any accident conditions. The numerical calculation of TASFIS has been performed by using ADI (Alternating direction–implicit) scheme, which is probably the most popular method for solving the incompressible flow problems.

Even though the boiling is permitted under any condition IV incidents, such as the complete loss of forced cooling, one of the thermal design criteria for the underwater storage and the design concept for the abnormal maximum heat load are to preclude the boiling of pool water, because these faults have the possibility of the release of radioactive material which exceeds the acceptable amount of 10CFR100.[12] The temperature limitations of the pool water is thus used as a basis for meeting this criterion. The limiting conditions for the compacted spent fuel storage, by varying the various major parameters, have been found to confirm the safety assurance of the rod consolidation method.

2. Theoretical Considerations

The simplified schematic diagram of the spent fuel pool storage is depicted in Fig.1. As shown in the figure, the fuel rod array is bounded on each fuel assembly or rack of its lateral extremities by a vertical wall of height L. The one function of the vertical bounding walls is to create a pressure head to induce a vertical upward flow through the fuel rod channel, and the other is expressed with the driving force coming from the temperature difference between the channel and ambient water. The flow rate is established by a dynamic balance between the buoyancy force and the friction force.[13]

The fuel element arrays determine the geometric configuration in which TASFIS can model the entire pool. The primary flow cell may be used to represent the pool if one were interested in the ambient temperature and pressure of the medium. The major assumptions for deriving the governing equations are as follows;

(1) The coolant is single phase and laminar flow with Rayleigh Number $(Ra_D) \leq 10^5$.

(2) The coolant flow has an axially predominant convection, thus only the axial velocity is considered.

(3) The heat balance in the spent fuel pool by a steady state calculation, is used to determine the temperature evolution. The ambient equilibrium pool temperature is assumed to be a maximum value of 150°F, as recommended in ANS–57.2, ANSI N210–1976.

(4) The Boussinesq approximation is valid[14], thus the fluid is assumed to be incompressible except for the buoyancy term in the vertical direction.

(5) All other physical properties are constant, because these variations are negligible within the acceptable ranges, except the density of

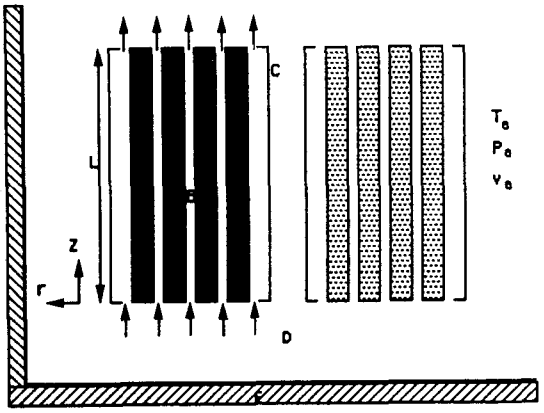

Fig. 1. Schematic Diagram of Spent Fuel Pool Storage Configuration and Natural Circulation Flow
(A) Spent Fuel Element
(B) Flow Channel
(C) Assembly Wall
(D) Ambient Water
(E) Concrete Encasement or Pool Structure

the buoyancy term and the temperature-dependent viscosity.

(6) The heat removal mechanism from the pool storage and assembly walls is neglected due to their small increment to the natural convection. Thus, the modeling is only made to the spent fuel rod geometry, which gives the simplified boundaries and some conservative results.

Clearly, since the fluid motion is caused by the density variations, we must take into account the temperature dependency of the density if we were intended to analyze natural convection phenomena. TASFIS can be applicable to liquid or gas cooled systems as long as the above assumption of constant fluid properties is valid. It is modeled that the primitive variables, i.e. the density, the axial velocity, and the pressure are splited into two parts as an ambient part (subscript of a) and a perturbed part (script of ′) as follows;

$$\rho = \rho_a + \rho' \quad (\text{where } \rho' \ll \rho_a) \tag{1}$$

$$v = v_a + v' \quad (\text{where } v_a \fallingdotseq 0) \tag{2}$$

$$p = p_a + p' \quad (\text{where } \nabla p_a \ll \rho_a g) \tag{3}$$

Under the above assumptions and the Boussinesq equation of state from the following equation of

$$\rho' g = -\rho_a \beta (T - T_a) g, \tag{4}$$

the governing equations were obtained as follows, which describe the transient axial flow and heat transfer in a viscous incompressible fluid occupying the flow cells. The viscous dissipation and reversible work terms are ignored due to their small affects.

Continuity Equation : $\partial v'/\partial z = 0$ (5)

Equation of Motion :

$$\rho_a\left(\frac{\partial v'}{\partial \tau} + v'\frac{\partial v'}{\partial z}\right) = -\frac{\partial p'}{\partial z} + \rho_a \beta g(T-T_a) + \mu\nabla^2 v' + \nabla\mu\frac{\partial v'}{\partial z} \tag{6}$$

where

$$\mu = \mu_a \left[1 + 1/\mu_a \left(\frac{\partial \mu}{\partial T}\right)_a (T - T_a) \right]$$

$$\nabla\mu = \left(\frac{\partial \mu}{\partial T}\right) / \frac{\partial T}{\partial z}$$

Energy Equation :

$$\frac{\partial T}{\partial \tau} + v' \frac{\partial T}{\partial z} = \alpha \nabla^2 T + \frac{\phi}{\rho_a Cp} \tag{7}$$

where

α = thermal diffusivity of the fluid

ϕ = source term

Also by introducing the following dimensionless numbers and variables,

$$Gr_L = \beta g (T_0 - T_a) L^3 / \nu_a^2, \quad Pr = \nu_a / \alpha, \quad R = r/S,$$

$$Z = z/L, \quad V = Lv'/\nu_a, \quad \omega = (T - T_a)/(T_0 - T_a),$$

$$t = \tau \nu_a / L^2, \text{ and } P = p' \beta_a L^2 / \mu_a^2,$$

the governing equations have the dimensionless forms as follows ;

$$\partial V / \partial Z = 0 \tag{8}$$

$$\frac{\partial V}{\partial t} + V \frac{\partial V}{\partial Z} = -\frac{\partial P}{\partial Z} + Gr_L \omega + (1 + \Lambda\omega)\nabla^2 V + \Lambda \frac{\partial \omega}{\partial Z}\frac{\partial V}{\partial Z} \tag{9}$$

$$\frac{\partial \omega}{\partial t} + V \frac{\partial \omega}{\partial Z} = \frac{1}{Pr} \nabla^2 \omega + \psi \tag{10}$$

where

$$\Lambda = 1 / \mu_a \left(\frac{\partial \mu}{\partial \omega}\right)_a \fallingdotseq \mu_0 / \mu_a - 1$$

$$\psi = \frac{\phi L^2}{\mu_a C_p (T_0 - T_a)}$$

Note that the specified dimensionless parameters are expressed as the coefficient of the non-dimensional terms, and that they show the relative importance of various terms in the equations. For example, the introduced characteristic velocity, ν_a/L, signifies that there is a relationship between

the shear force term and the inertia force term, and it implies the relative degree of order in the axial region of length L.

Initially, the fuel rod surface and the fluid are assumed to have an ambient temperature T_a, same as the inlet water temperature, and are supposed to have zero velocity (no motion). The boundary conditions relevant to the rod bundle arrays are symmetric as shown in Fig.2. Owing to the symmetry, only the domain of $0<\theta<\theta_0$ is selected, and it is called a primary flow cell. The transformed boundary conditions applied to the governing equations are given as follows, where the continuity equation is originally satisfied at inlet and outlet nodes.

1) the symmetric and adiabatic boundaries :

$$\partial V/\partial\theta = 0, \quad \partial\omega/\partial\theta = 0, \qquad \text{at } \theta = 0, \theta_0$$

$$\partial V/\partial Z = 0, \quad \partial\omega/\partial Z = 0, \qquad \text{at } Z = 1$$

$$R\,\partial V/\partial R = (\partial V/\partial\theta)\tan\theta \text{ and}$$

$$R\,\partial\omega/\partial R = (\partial\omega/\partial\theta)\tan\theta, \qquad \text{at } R = \sec\theta$$

2) no slip walls :

$$V = 0, \qquad \text{at } R = r_0/S$$

3) surface teat flux(Fourier's heat conduction Equation) :

$$\partial\omega/\partial R = -q''(\theta,Z)/k_f, \qquad \text{at } R = r_0/S$$

4) constant inlet temperature :

$$T_m = 0, \qquad \text{at } Z = 0$$

5) no pressure variation :

$$P = 0, \qquad \text{at } Z = 0, 1$$

3. Numerical Scheme

The differential equations were transformed into the finite difference form by integrating over a control volume surrounding each node or center point. This approach facilitates the expression of finite differences in more than one dimension and on curvilinear meshes. The nonlinear term in the equation of motion was linearized by adapting the Briley–McDonald method which is supposed to have the second order accuracy. Also the convection term in the energy equation was represented with the scheme of upwind differentiation in order to get the positive coefficients within the matrix algorithm. [17]

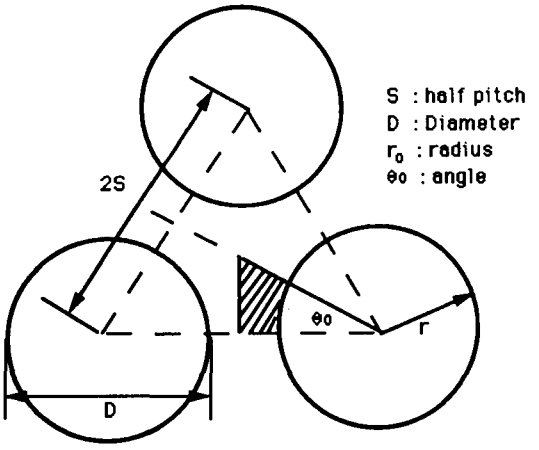

Fig. 2. Cross Section of a Three–rod Portion of Bundle Having an Equilateral Triangular Arrangement (Cross–hatched area Represents a Primary Flow Cell.)

The surface points in the primary flow cell was shifted one–half an increment for the adequate boundary conditions. To specify the values of the first derivative at the boundary, $r=r_0$ and $r=S/\cos\theta$, artificial points outside the region were assumed. A staggered grid for the pressure component was used, so that the pressure difference between two adjacent grid points gives the natural driving force for the velocity component located between these grid points. Forward differences for time derivatives and the second–order central differences for the spatial derivative of temperature and velocity were used. The resulting finite–difference equations were solved using the ADI method developed by Douglas and Peaceman for conduction and adopted later by H. S. Chu et al. [16], K.

Aziz et al.,[17] and A. J. Chorin.[18] The ADI method for the equations may be written in the form of three-step TDMA(Tri-Diagonal Matrix Algorithm) as ;

$$[\Lambda]^{\circ}[\Omega]=[\Phi] \tag{11}$$

where $[\Lambda]$ and $[\Phi]$ represent the matrix and source terms, respectively, which contains the calculated variables of the previous step. These three-step ADI schemes, which was implemented in TASFIS code, are second-order accurate and are unconditionally stable.

To solve the incompressible Navier-Stokes equation in primitive variable forms, the first step of the numerical iteration scheme is to find the guessed pressure such that the resultant transient velocity field will progressively get closer to satisfy the continuity equation. Either the artificial compressibility method developed by Chorin or the SIMPLE (Semi-Implicit Method for Pressure Linked Equations) procedure by Patankar and Spalding [19] is very useful for this purpose. The SIMPLE procedure, adopted in this numerical scheme, is based on a cyclic series of guess-of-correct operations to solve the governing equations. In this procedure, the actual variables were written as

$$p=p^{\vee}+p',\ v=v^{\vee}+v' \tag{12}$$

where $p^{\vee}$ and p' is called the guessed pressure and pressure correction term, respectively. Next, the pressure corrections were related to the velocity corrections by approximated dimensionless forms of the equation of motion, which results in the Poisson equation for the pressure correction because of the continuity constraint as follows ;

$$\partial V'/\partial t=-\partial P/\partial Z \tag{13}$$

with the boundary condition $P'=0$ at inlet and outlet nodes. From the Eq. (13) we developed an iteration scheme with a under-relaxation parameter. Note that if the estimated velocity vector satisfies continuity at every point, the pressure correction term goes to zero at every point, thus we terminate this iteration if the predetermined accuracy were obtained.

Decay heat, generated by spent fuel elements, varies strongly with the cooling time after its removal from the core, as well as the operating conditions and burnup experienced in the core - i.e. fuel cycle and neutronic energy spectrum. The major decay sources are fission products and the actinides, however, during cooling times less than few hundred years, the latter contributes much less to the decay heat than the former. The ANS-79 method was adopted to obtain the decay heat power with arbitrary reactor operating histories.[20] To characterize the variation of decay power along the axis of fuel rod, a chopped sine curve having a peak-to-average variation of 1.5 was assumed. It is considered that all rods in a fuel assembly have the same decay power variation ; decay heat generated in the fuel rods is transferred radially to the coolant. The mean surface heat flux from fuel rod to coolant is related to the decay heat generation rate and is necessary as initial condition for the numerical iteration scheme. However both the fuel rod surface temperature and the surface heat flux have the function of circumferential and axial position due to their dependency on coolant velocity.

Because the radial heat conduction is greater than the axial conduction by several orders of magnitude, the axial conduction for the oxide fuel was neglected. The steady state energy equation with a negligible circumferential heat conduction for fuel rod was also utilized to overcome the required mesh generation in the solid region. To calculate temperatures, velocities and pressures at a new time step from the values at the previous time step, the following computational cycle was followed.

1) Initialization : When the appropriate meshes are generated in primary flow cell and the artificial boundaries, and the grid sizes are settled, the

calculations are started with initial conditions of uniform inlet temperature, no motion, and no pressure condition, as well as the uniform heat flux.

2) The new temperature field is computed by solving in tridiagonal form the finite approximations of equations for the three time steps.
3) The surface temperature is computed from the boundary condition, i.e. Fourier s heat conduction equation. Using the calculated surface temperature, the center-line temperatures are obtained from the heat conduction formula in solid region. With the new center-line and surface temperatures of rod, the heat flux can be recalculated and they are normalized based on the mean heat flux.
4) With the calculated temperature field, the new velocity field is computed from the three-step tri-diagonal forms.
5) The pressure correction equation with the new velocity field is solved. The velocity and pressure from the iteration scheme is also adjusted until the convergence criteria is satisfied.
6) The new corrected temperature, velocities and pressures with the starting values are replaced for the next time step cycle. It is repeated the above whole process from Number 2 to Number 5 until the steady state values are obtained.

4. Results and Discussion

Various parametric study for the natural convection flow in the rod consolidation method was successfully performed. Even though the ADI schemes are unconditionally stable, an optimum time size is generally necessary to solve the coupled, nonlinear problems and must be found to be satisfactory. The global discretization error would depend to a certain extent on how to treat the nonlinear terms and the number of iteration performed at each step. It is found desirable to regulate the time size to avoid numerical oscillations, as Rayleigh number Ra_D, i.e. the hydraulic diameter D_e , increased as remarked by Chu. [16] It is defined in the following form.

$$D_e = 2r_o[(S/r_o)^2 \cdot \tan \theta_o/\theta_o - 1] \quad (14)$$

The axial temperature profiles at the surface of the fuel rod and the coolant with mean value are shown in Fig.3. The maximum surface and bulk temperature of the fuel rod are at the exit of the channel. The temperature difference between this mean surface temperature and the bulk temperature will be used in defining the local convective heat transfer coefficient. The significant comparison was carried out between the triangular and rectangular array under the same conditions. The effluent temperature of the triangular type of the fuel rods is higher than that of the rectangular type by about 15℃. This is due to the fact that the dependence of the heat transfer results upon geometrical parameters, especially the hydraulic diameter. As the ratio of hydraulic diameter to rod diameter, $D_e/2r_o$ as defined in Eq.(14), is increased from 0.334 for triangular array to 0.541 for rectangular array, for the case of $S/r_o = 1.1$ and the same radius, the power density of the

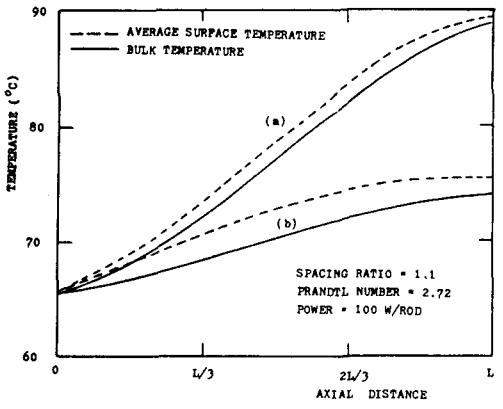

Fig. 3. Axial Bulk Temperature and Average Surface Temperature Profiles. (a) Triangular Array (b) Rectangular Array

latter is decreased by the factor of 0.62 than that of the former. It was proved because the cross-sectional area of the fluid holding an equal amount of one fuel rod heat generation is represented as follows;

$$A_c = \pi r_o^2 (D_e/2r_o). \quad (15)$$

Thus from the Eq.(15), it can be predicted that as the hydraulic diameter or the radius of fuel rod increased, the effluent temperature will be decreased. At the normal condition with the functioning of cooling pumps, the employment of the triangular array for the rod consolidation design will be very likely desired because of its higher heat transfer characteristic, and the storage capacity can be more achieved than the rectangular array for the typical LWR fuel assembly. But as for the accident condition, as indicated in Fig.3, the latter will be desirable because of its underheating effect of the system.

The calculated velocity contours with respect to the spacing ratio are shown in the Fig.4(a) and Fig.4(b) for Prandtl number of 2.72. As shown in figures, the relative velocity to the average flow velocity at any radial and angular points is found in the domains. It is known that the value of relative velocity is independent of the variation of the decay heat generation. As indicated in figures, the wide variations are more revealed according to the decreasing spacing ratio, which suggests the need of the three-dimensional calculation immanently as long as the spacing ratio is decreased.

Fig.5 is a plotting for the ratio of the peripheral heat flux to the mean heat flux versus the angular position at mid-length of fuel rod. Its result was compared with the analytical solution by E. M. Sparrow [21] through the consideration of same boundary condition. The result was accomplished with the assumptions of fully developed flow and heat transfer, for an open bundle. He adopted the

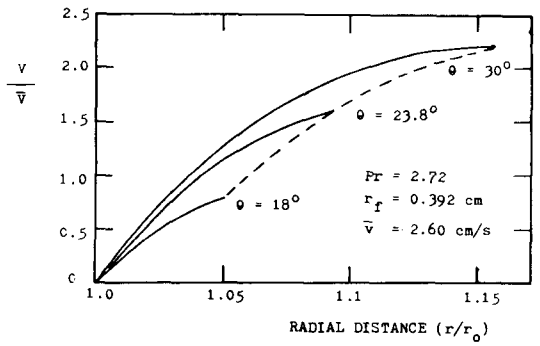

Fig. 4a. Radial Velocity Distribution with Spacing Ratio of 1.0

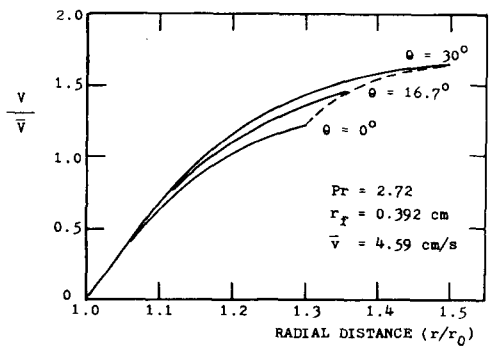

Fig. 4b. Radial Velocity Distribution with Spacing Ratio of 1.3

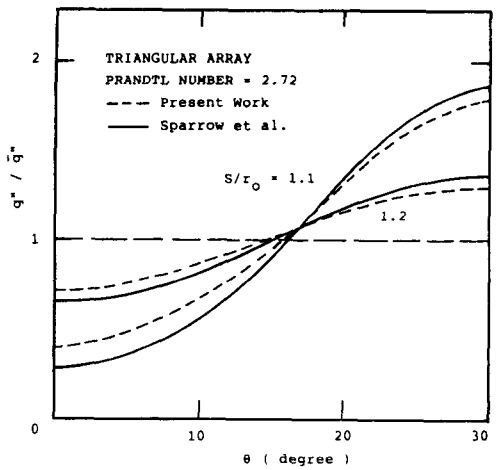

Fig. 5. Peripheral Variation of Local Wall Heat Flux at Midlength of Fuel Rod, Compared with the Result of Ref. 20

boundary conditions of uniform wall temperatures in the circumferential direction and uniform wall heat flux in the axial direction. The admissible agreement between TASFIS and analytical solution was obtained. It can be seen from Fig.5 that the largest heat transfer occurs at $\theta=30$℃, location of the most open area for flow, because of the geometrical characteristic.

Fig.6 and Fig.7 show the effluent bulk temperature and average velocity with regard to the decay heat generation from a typical fuel rod having fuel inner radius of 0.392 centimeter. Fig.6 shows the effluent temperature, with spacing ratio of 1.1, can be exceeded 100℃ when the heat power is 220 watts (W) per unit fuel rod. Fig.7, the case of the closest compacted state, also indicates that the effluent bulk temperature will be 100℃ when the heat power is 42 W per fuel rod. The minimum coverage of 10 feet pool level above the fuel assembly, as requested in reference 4, is required to protect plant personnel during fuel loading and transfer operations. If the top of the spent fuel assembly were located with the sufficient depth from the surface, the boiling temperature of the effluent water would be increased to 107℃. For that effluent water temperature, the decay heat power of the spent fuel will be 63 W per unit rod as shown in Fig.7. From the comparison between Fig.6 and Fig.7, we can predict that the effluent bulk temperature is abruptly decreased as the spacing ratio is increased. Fig.8 will be used to confirm this prediction. The bulk boiling occurs from the compacted state in atmospheric condition at about the decay heat of 63 W per unit rod is loaded with spacing ratio of 1.02. Fig.9 shows the effluent bulk temperature and average velocity with regard to the radius of fuel rod. It was mentioned previously that the effluent bulk tempera-

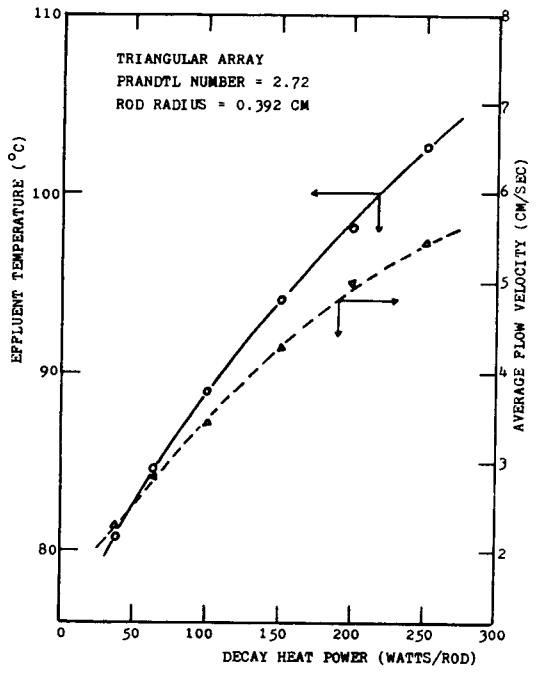

Fig. 6. Effluent Bulk Temperature and Average Flow Velocity vs. the Decay Heat Power (Spacing Ratio=1.1)

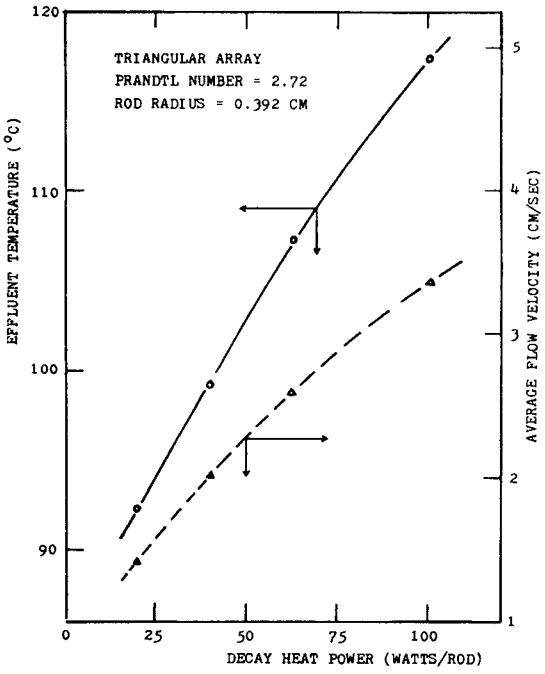

Fig. 7. Effluent Bulk Temperature and Average Flow Velocity vs. the Decay Heat Power (Spacing Ratio=1.0)

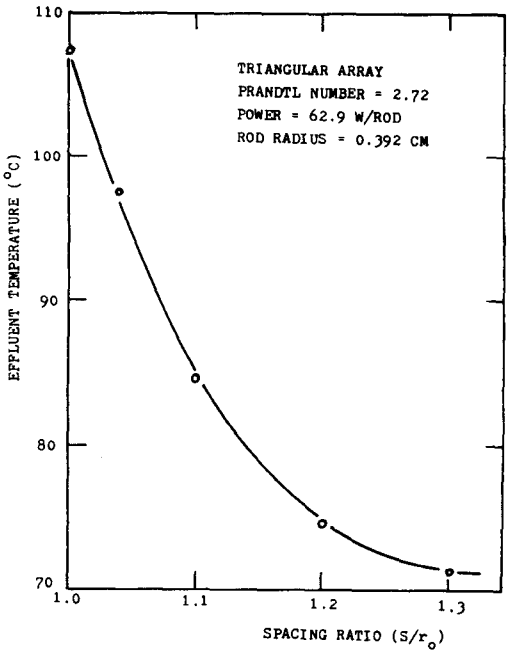

Fig. 8. Effluent Bulk Temperature vs. Spacing Ratio for the Decay Heat Power of 62.9 W/rod

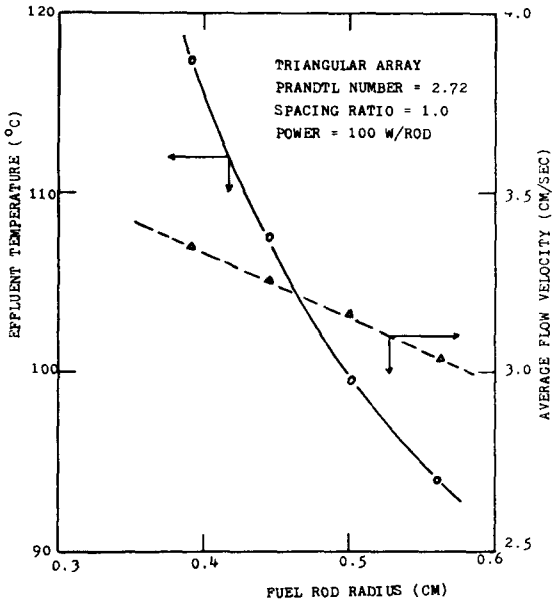

Fig. 9. Effluent Bulk Temperature and Average Flow Velocity Concerning About the Variation of Fuel Rod Radius

ture is decreased as the increase of the spacing ratio or the radius of fuel rod. Fig.9, as well as Fig.8, shows that this prediction has a sufficient evidence.

The fraction of decay power to normal full power with regard to the cooling time was calculated by using of ANS–79 model to provide the insights on the sufficient cooling times. From the above results, the required cooling time to preclude the bulk boiling in the pool with rod consolidation will be obtained for the actual design cases. For example, it is considered that the triangular arrays of most compacted state are loaded after the refueling at Kori–3/4 NPPs with a rated power of 2775 MWt. From the adoption of the standard fuel design data with fuel rod radius of 0.392 cm, the required cooling time to prevent the bulk boiling at the normal pool capacity would be about 162 days for the rod consolidation system.

5. Conclusion

In order to assess the cooling capability in the consolidated spent fuel pool for laminar, buoyancy induced flow, the implicit finite difference equations have been formulated, which implemented in the own–developed code, i.e. TASFIS. Some characteristics for the heat transfer mechanism were found with the parametric study on the configurations of the fuel rod and the storage types, which are as follows;

- It is confirmed that the three dimensional calculation will be required as long as the inter–fuel spacing ratio for the compacted storage is decreased.
- The triangular type of arrays in the most compacted state, as well as with the small radius of fuel rod, are more likely to initiate the bulk boiling in the spent fuel pool with the natural circulation than that of the rectangular type.
- The acceptance criteria required for the minimum cooling time were achieved for the pre-

vention of the pool bulk boiling in the compacted spent fuel storage system.

Nomenclature

A_c Cross-sectional Area of Flow Channel
C_p Specific Heat of the Fluid
D_e Hydraulic Diameter
Gr^L Grashof Numbder with the Characteristic Length of L
g Gravitational Acceleration
k_f Thermal Conductivity of Fuel
L Length of Fuel Rod
P Pressure (dimensionless)
p Pressure
Pr Prandtl Number
q'' Surface Heat Flux
Ra_D Rayleigh number with the Characteristic Length of D_e
R Radial Coordinate (dimensionless)
r Radial Coordinate
r_o Outer Radius of Fuel Rod
S Half of Pitch Distance
t Time (dimensionless)
To Reference Temperature in the Pool Environment
T_{in} Inlet Temperature of the Flow Channel
V Velocity (dimensionless)
v Velocity
Z Vertical Coordinate (dimensionless)
z Vertical Coordinate
α Thermal Diffusivity
β Coefficient of Thermal Expansion
θ Angular Coordinate
θ_o Angle of Equilateral Triangle
μ Coefficient of Shear Viscosity
ρ Density of the Fluid
τ Time
ϕ Rate of Heat Generation
ψ Rate of Heat Generation (dimensionless)
ω Temperature (dimensionless)
$\wedge$ Viscosity Ratio
Λ Matrix Term in the Tri-diagonal Matrix Formula
Φ Source Term in the Tri-diagonal Matrix Formula
Ω Variable Term in the Tri-diagonal Matrix Formula

References

1. A.B. Johnson, Jr., "Spent Fuel Storage Experience", *Nucl. Technol.*, **43**, 165-173 (1978)
2. KRC-84N-T18, "Study on an Interim Storage of Spent Fuels", KAERI (1985)
3. Wayne L. Dobson et al., "Interim Spent Fuel Storage Using Rod Consolidation", *Trans. ANS*, **46**, 105 (1984)
4. "Spent Fuel Pool Cooling and Cleanup System", Standard Review Plan, Ch.9.1.3, U.S. NRC, July (1981)
5. A.S. Benjamin et al., "Spent Fuel Heatup Following Loss of Water During Storage", *Nucl. Technol.*, **49**, 274-294 (1980)
6. M.E. Weech et al., "Heat Transfer in Spent Fuel Storage", *Nuclear Eng. and Design*, **67**, 379-389 (1981)
7. R.L. Moscardini, "Fuel Consolidation Program Progress Report", Waste Management, CE Power Sys., March (1985)
8. DOE/ET/47912-4, "Safety Analysis Report Supplement for Consolidated Fuel Rod Storage at an Independent Spent Fuel Storage Installation", Volume IV, Sep. (1981)
9. J.M. Wu et al., "Three-Dimensional Numerical Analysis of Natural Convection of Compacted Spent Fuel", *Nucl. Technol.*, **63**, 40 (1983)
10. C.L. Wheeler, D. S. Rowe et al., "COBRA-IV-I ; An Interim Version of COBRA for Thermal-Hydraulic Analysis of Rod Bundle Nuclear Fuel Elements and Cores", BNWL-1962, Mar. (1976)
11. H. Chelemer, P.T. Chu et al., "THINC-IV ;

An Improved Program for Thermal Hydraulic Analysis of Rod Bundle Cores", WCAP-7956, June (1973)

12. "Design Objectives for Light Water Reactor Spent-Fuel Storage Facilities at Nuclear Power Stations", ANS-57.2, ANSI N210-1976, American Nuclear Society (1976)
13. E.M. Sparrow and C. Prakash, "Enhancement of Natural Convection Heat Transfer by a Staggered Array of Discrete Vertical Plates", *J. of Heat Transfer,* **102**, 215-220, May (1980)
14. D. D. Gray et al., "The Validity of the Boussinesq for Liquids and Gases", *Int. J. of Heat & Mass Transfer,* **19**, pp.545- 551 (1976)
15. P.J. Roache and T.J. Mueller, "Numerical Solutions of Laminar Separated Flows, *AIAA J.,* **8**, No.3, 530-538 (1970)
16. H.S. Chu et al., "The Effect of Heater Size, Location, Aspect Ratio, and Boundary Conditions on Two-Dimensional, Laminar, Natural Convection in Rectangular Channels", *J. of Heat Transfer,* **98**, 194 (1976)
17. K. Aziz et al., "Numerical Solution of the Three-Dimensional Equations of Motion for Laminar Natural Convection", *Physics of Fluids,* **10**, No.2, 314-324 (1967)
18. A.J. Chorin, "Numerical Solution of the Navier-Stokes Equations", *Math. Computation,* **22**, 745-762 (1968)
19. S.V. Patankar, Numerical Heat Transfer and Fluid Flow, McGraw-Hill Book Company (1980)
20. V.E. Schrock, "A Revised ANS Standard for Decay Heat from Fission Products", *Nucl. Technol.,* **46**, 323-331 (1979)
21. E.M. Sparrow et al., "Heat Transfer to Longitudinal Laminar Flow Between Cylinders", *J. of Heat Transfer,* **83**, 415-422, (1961)